HIGH FREQUENCY APPROXIMATIONS TO MULTIPLE SCATTER BY ROUGH SURFACES THAT EXHIBIT ENHANCED BACKSCATTER.

E. Bahar and M. El-Shenawee

Electrical Engineering Department, University of Nebraska-Lincoln
Lincoln, NE 68588-0511, U.S.A.

Abstract - Integral expressions for the single and double scattered radar cross sections are obtained using the full wave approach. The surface heights and slopes at two points on the random rough surface are characterized by Gaussian joint probability density functions. The surface height autocorrelation function and its Fourier transform (the rough surface spectral density function) are also assumed to be Gaussian. Two and six dimensional integral expressions are obtained for the single and double scattered cross sections. They account for the correlations between the heights and the slopes of the random rough surface. The high frequency approximations reduce the expressions for the double scatter cross sections from six to two dimensional integrals. The results show that the enhanced backscatter is due to multiple scatter from rough surfaces with large mean square slopes and heights.

Keywords : Multiple Scatter - Enhanced Backscatter - Full wave.

FORMULATION OF THE PROBLEM

The random rough surfaces are assumed to vary in one dimension only $y=h(x)$. The full wave double scattered far fields $G_d^f(\bar{r})$ are given by [1]

$$G_d^f(\bar{r})=\frac{k_o^2}{4\pi^2}\sqrt{\frac{2\pi}{k_o r}}\,e^{j\pi/4}\,e^{-jk_o r}\int D_2(\bar{n}^f,\bar{n}')\,D_1(\bar{n}',\bar{n}^i)$$
$$\cdot\exp\{jk_o(\bar{n}^f\cdot\bar{r}'_{s2}-\bar{n}^i\cdot\bar{r}'_{s1}-\bar{n}'\cdot\bar{r}'_{21})\}\,U(\bar{r}'_{s1})\,U(\bar{r}'_{s2})$$
$$\cdot\frac{dn'_y}{n'_x}\,dx'_{s1}\,dx'_{s2}\,G^i(0) \qquad (1a)$$

in which $\bar{n}^i$ and $\bar{n}^f$, the unit vectors in the directions of the incident and scattered fields are, respectively.

$$\bar{n}^i=n_x^i\,\bar{a}_x+n_y^i\,\bar{a}_y, \qquad \bar{n}^f=n_x^f\,\bar{a}_x+n_y^f\,\bar{a}_y \qquad (1b)$$

and $\exp(j\omega t)$ time excitations are assumed. The wave vector for the fields scattered from the surface at $\bar{r}'_{s1}$ to the surface at $\bar{r}'_{s2}$ is in the direction of the unit vector $\bar{n}'$ (see fig.1). The free space wave number is $k_o=\omega\sqrt{\mu_o\epsilon_o}$. The scattering coefficients at points 1' and 2' on the surface are $D_1(\bar{n}',\bar{n}^i)$ and $D_2(\bar{n}^f,\bar{n}')$, respectively. The scattering coefficients depend on the polarization of the incident and scattered waves, the media on both sides of the rough interface, and the local normals $\bar{n}'_1$ and $\bar{n}'_2$ at points 1' and 2', respectively. The quantities $G^i(0)$ and $G_d^f(\bar{r})$ are the vertically or the horizontally polarized field components of the incident and scattered waves, respectively. At high frequencies, the shadow function $U(\bar{r}'_{s1})$ is equal to one if the point at $\bar{r}'_{s1}$ is illuminated by the incident wave and visible by the point at $\bar{r}'_{s2}$. The shadow function $U(\bar{r}'_{s2})$ is equal to one if the point at $\bar{r}'_{s2}$ is illuminated by a source at $\bar{r}'_{s1}$ and visible to the receiver [2]. For one dimensionally rough surfaces

$$\bar{r}'_{s1}=x'_{s1}\bar{a}_x+h(x'_{s1})\bar{a}_y, \qquad \bar{r}'_{s2}=x'_{s2}\bar{a}_x+h(x'_{s2})\bar{a}_y,$$
$$\bar{r}'_{21}=\bar{r}'_{s2}-\bar{r}'_{s1}, \qquad \bar{n}'=n'_x\bar{a}_x+n'_y\bar{a}_y \qquad (1c)$$

The double scatter intensity is obtained by multiplying the expression for the field (1a) by its complex conjugate $G_d^f(\bar{r})^*$ (see fig.2). It is assumed that $k_o\rho\gg 1$, where k_o is the free space wave number and ρ is the radius of curvature of the rough surface. It is also assumed that the Raleigh parameter is large, $\beta=(\bar{v}\cdot\bar{a}_y)^2\langle h^2\rangle\gg 1$, where $\langle h^2\rangle$ is the mean square height, $\bar{v}=k_o(\bar{n}^f-\bar{n}^i)$ and $\bar{a}_y$ is the unit vector normal to the mean surface. The statistical averages of the intensities with respect to the random heights and slopes at two pairs of points on the surface involve conditional joint characteristic functions [3]. At high frequencies the Fourier transform of the conditional joint characteristic function is proportional to the Dirac delta functions of the slopes at the specular points, independent of the statistical characterization of the surface. Using the high frequency approximations, the six dimensional integral expressions for the double scatter intensities reduce to two dimensional integrals over the scatter wave vector variables n'_y and n''_y. Thus in the high frequency limit, the major contributions to the double scattered cross sections come from the neighborhoods of the specular points of the surface.

The significant contributions to the double scattered intensities come from two different double scatter paths, the quasi parallel, regular path (see fig.2-a) and the quasi anti-parallel, cross path (see fig.2-b). In figs.2-a,b the scatter wave vectors from points 1' and 1'' on the rough surface to points 2' and 2'' on the surface are in the direction of the unit vector $\bar{n}'$ and $\bar{n}''$, respectively. The double scatter cross section associated with the parallel path is given by

$$\langle\sigma_{regular}\rangle=4\int_{\theta'=-\pi}^{\pi}\int_{\theta''=-\pi}^{\pi}\Big[\!\Big[\frac{D_2(\bar{n}^f,\bar{n}')\,D_1(\bar{n}',\bar{n}^i)\,D_2^*(\bar{n}^f,\bar{n}'')\,D_1^*(\bar{n}'',\bar{n}^i)}{[-2n_y^i+(n'_y+n''_y)]\,[2n_y^f-(n'_y+n''_y)]}$$
$$\cdot p(h_{x1})\,p(h_{x2})\exp\{-k_o^2\langle h^2\rangle(n''_y-n'_y)^2\}(2k_oL_m)$$
$$\cdot\operatorname{sinc}\{k_oL_m(n''_x-n'_x)\}\Big]\!\Big]_{h_{x1}=h_{x1s},\;h_{x2}=h_{x2s}}$$
$$\cdot[1-P_2(|n'_y|)]\,[1-P_2(|n''_y|)]\,d\theta'\,d\theta''\,P_2(\bar{n}^i)\,P_2(\bar{n}^f) \qquad (3a)$$

where

$$n'_y=\cos\theta',\quad n'_x=\sin\theta',\quad n''_y=\cos\theta'',\quad n''_x=\sin\theta'' \qquad (3b)$$

and

$$h_{x1s}=\frac{-[-n_x^i+(n'_x+n''_x)/2]}{[-n_y^i+(n'_y+n''_y)/2]}, \qquad h_{x2s}=\frac{-[n_x^f-(n'_x+n''_x)/2]}{[n_y^f-(n'_y+n''_y)/2]} \qquad (3c)$$

In (3), $P_2(|n'_y|)$ and $P_2(|n''_y|)$ are the probabilities that no part of the surface will intersect the rays in the directions of the wave vectors $\bar{n}'$ and $\bar{n}''$ upon scattering by the surface at points 1' and 1'', respectively [2]. Thus $([1-P_2(|n'_y|)]\,[1-P_2(|n''_y|)])$ is the probability that the single scattered field will intersect the surface in the direction of the wave vectors $\bar{n}'$ and $\bar{n}''$. It represents the probability for multiple scatter to occur. The probabilities that the surface will not intersect the incident and the scattered waves are given by $P_2(\bar{n}^i)$ and $P_2(\bar{n}^f)$, respectively [2]. The distance L_m is the mean path for the double scattered wave. The probability density functions for the slopes at two points on the double scatter path are given by $p(h_{x1})$ and $p(h_{x2})$. The slopes at the specular (stationary phase) points are h_{x1s} and h_{x2s}. The angles between the unit vectors $\bar{n}'$ and $\bar{n}''$ and the vertical y-direction are θ' and θ'', respectively.

Similarly, the double scatter cross section for the cross (anti-parallel) path (see fig.2b) is given by

$$\langle\sigma_{cross}\rangle=4\int_{\theta'=-\pi}^{\pi}\int_{\theta''=-\pi}^{\pi}\Big[\frac{D_2(\bar{n}^f,\bar{n}')\,D_1(\bar{n}',\bar{n}^i)\,D_2^*(\bar{n}'',\bar{n}^i)\,D_1^*(\bar{n}^f,\bar{n}'')}{[n_y^f-n_y^i-n_y'+n_y'']\,[n_y^f-n_y^i+n_y'-n_y'']}$$

$$\cdot p(h_{x1})\,p(h_{x2})\exp\{-k_o^2\langle h^2\rangle(n_y^f+n_y^i-n_y''-n_y')^2\}$$

$$\cdot(2k_oL_m)\,\mathrm{sinc}\{k_oL_m(n_x^f+n_x^i-n_x''n_x')\}\Big]_{h_{x1}=h_{x1s},h_{x2}=h_{x2s}}$$

$$\cdot[1-P_2(|n_y'|)]\,[1-P_2(|n_y''|)]\,d\theta'\,d\theta''\,P_2(\bar{n}^i)\,P_2(\bar{n}^f) \qquad (4a)$$

where

$$h_{x1s}=\frac{-[n_x^f-n_x^i+n_x'-n_x'']}{[n_y^f-n_y^i+n_y'-n_y'']},\qquad h_{x2s}=\frac{-[n_x^f-n_x^i-n_x'+n_x'']}{[n_y^f-n_y^i-n_y'+n_y'']} \qquad (4b)$$

Note that the denominators of (3a) and (4a) vanish only if the slopes at the specular points are infinite. For these cases $p(h_{x1})\rightarrow 0$ and $p(h_{x2})\rightarrow 0$ and the integrand remains finite. It is found that the sharp enhanced backscatter, which is due to the contribution of the cross term (4) in the expression for the double scatter cross section, occurs when the rough surface mean square height and slope are large ($\langle h_x^2\rangle \geq 0.5$ and $4k_o^2\langle h^2\rangle \geq 40$). In this case the correlation length is of the order of the rms height. The total incoherent cross section is the sum of the single and the double scatter (quasi parallel and quasi anti-parallel) cross sections.

ILLUSTRATIVE EXAMPLES

The integrands of the two dimensional integrals (3) and (4) are plotted in figs. 3 and 4 as functions of the angles θ' and θ'' (radians) between the unit vectors $\bar{n}'$ and $\bar{n}''$ and the y-axis. These integrands represent the contributions of the quasi parallel path and the quasi anti-parallel path. The rough surface mean square height is given by the Raleigh parameter $\beta=4k_o^2\langle h^2\rangle=41.077$, the mean square slope $\langle h_x^2\rangle=0.508$, and the mean double scatter path $L_m=11.13\ l_c$ (l_c is the correlation length). The relative permittivity is $\epsilon_r=-424.64-j81.144$ at the wave length $\lambda=3.392\ \mu m$. The incident wave is $\theta^i=10^\circ$ and $\phi^i=0$. In fig. 3 the scattered wave is in the direction $\theta^f=10^\circ$, $\phi^f=180^\circ$ (backscatter) and in fig. 4 $\theta^f=5^\circ$ and $\phi^f=180^\circ$. The major contributions to the quasi parallel path are along the diagonal ($\theta'=\theta''\approx\pm 90^\circ$) and the major contributions to the quasi anti-parallel path are along the anti-diagonal ($\theta'=-\theta''\approx\pm 90^\circ$). Note that the quasi parallel and the quasi anti-parallel contributions are equal (in the high frequency limit) for the backscatter case $\theta^i=\theta^f=10^\circ$ (fig. 3). However for $\theta^i=10^\circ$ and $\theta^f=5^\circ$ ($\phi^i-\phi^f=180^\circ$) the contributions from the quasi anti-parallel path become relatively small (fig. 4). In fig. 5 both the single and the double (quasi parallel and quasi anti-parallel) scatter cross sections are plotted as functions of the scatter angle θ^f (where $\phi^i-\phi^f=0,180^\circ$). For this case the parameters of the one dimensional rough surface are: $\beta=356.1287$, $\langle h_x^2\rangle=0.508$, $L_m=11.13\ l_c$, and $\epsilon_r=-62.787-j4.948$ ($\lambda=1.15\ \mu m$). The incident wave is $\theta^i=10^\circ$ and $\phi^i=0$. These results show that there are no significant differences between the vertically and the horizontally polarized waves when the high frequency approximations are used. The intensity fluctuations about the backscatter directions are due to interactions between the scattered intensities at the two points on the rough surface.

The full wave, six dimensional integrals (not given here) are also computed in a tractable manner after transforming the variables of integration. In fig. 6, the surface parameters are the same as in fig. 3 for the incident angle $\theta^i=10^\circ$ and $\phi^i=0$. The vertically and the horizontally polarized total (single+double) diffuse cross sections are plotted as functions of the scatter angle θ^f ($\phi^i-\phi^f=0,180^\circ$). These results for the six dimensional integrals, indicate that the double scattered fields are polarization dependent and the backscatter intensity does not drop as sharply about the backscatter direction as implied by the high frequency approximations. Parametric curves are plotted in figs. 7, and 8 for the vertically polarized double scatter cross sections as functions of the scatter angles θ^f ($\phi^i-\phi^f=0,180^\circ$).

For the results shown in fig.7, the rough surface parameters are: $\epsilon_r=-62.787-j4.948$ ($\lambda=1.15\ \mu m$), $\beta=4k_o^2\langle h^2\rangle=356.128$, and $\langle h_x^2\rangle = 0.508$. The incident wave is $\theta^i=10^\circ$ and $\phi^i=0$. The mean path for the double scattered wave L_m is 5.5 l_c, 11.13 l_c, 22 l_c, and 54 l_c. The enhanced backscatter intensity is maximum for $L_m\approx 22$ l_c. However the intensity does not vary significantly for L_m/l_c between 10 and 30. For the results shown in fig. 8, the surface parameters are: $\epsilon_r=-424.648-j81.14$ ($\lambda=3.39\ \mu m$), $\langle h_x^2\rangle=0.508$, and $L_m=11.13\ l_c$. The incident wave is $\theta^i=10^\circ$ and $\phi^i=0$. The Raleigh parameter β is varied from 3.0 (relatively smooth surface) to 300 (very rough surface). The results in fig. 8 show that the enhanced backscatter peak increases with β, however for $\beta>150$ there is no significant change. The width of the intensity about the backscatter direction becomes narrower as β increases. In fig. 9, the rough surface parameters are the same as in fig. 3 except that the mean square slope varies between 0.508 and 2. The total (single+double) diffuse incoherent vertically polarized cross sections are plotted as functions of the scatter angle θ^f ($\phi^i-\phi^f=180^\circ$). As the mean square slope increases, the enhanced backscatter cross sections increase. However the results do not differ significantly for $\langle h_x^2\rangle$ greater than one. For rough surfaces with maximum slopes less than 40°, the double scatter cross sections are insignificant compared to the single scatter cross sections.

ACKNOWLEDGMENT

The computational work was conducted at the Cornell National Supercomputer Facility. This work is partially supported by the Center for Electro-Optics at the University of Nebraska-Lincoln.

REFERENCES

[1] E. Bahar and M. El-Shenawee, "Use of supercomputers to evaluate singly and doubly scattered electromagnetic fields from rough surfaces," IEEE Trans. on Magnetics, vol. 27, no. 5, pp. 4287-4290, September 1991.

[2] B. G. Smith, "Geometrical Shadowing of a Random Rough Surface," IEEE Trans. Antenn. and Propag., vol. AP-S, no. 5, pp. 668-671, September 1967.

[3] E. Bahar, "Full Wave Analysis for Rough Surface Diffuse, Incoherent Radar Cross Sections with Height-Slope Correlations Included" IEEE Trans. Antenn. and Propag., vol. AP-S, no. 9, pp. 1293-1304, September 1991.

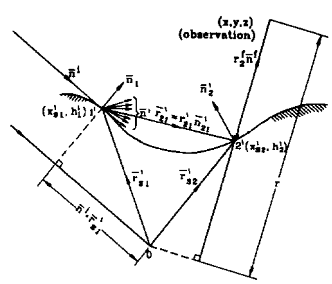

Fig.1 The double scattered electromagnetic waves.

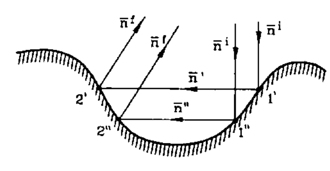

Fig.2-a Quasi-parallel, regular path $\bar{n}'\approx\bar{n}''$

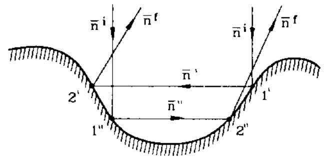

Fig.2-b Quasi-antiparallel, cross path $\bar{n}' \approx -\bar{n}''$

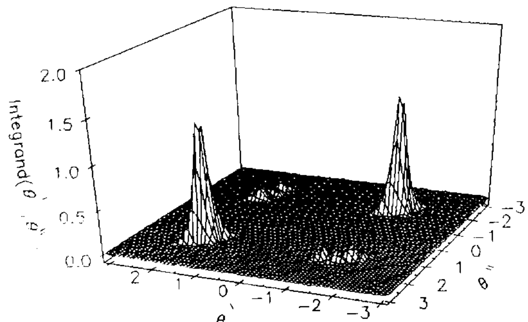

Fig.4

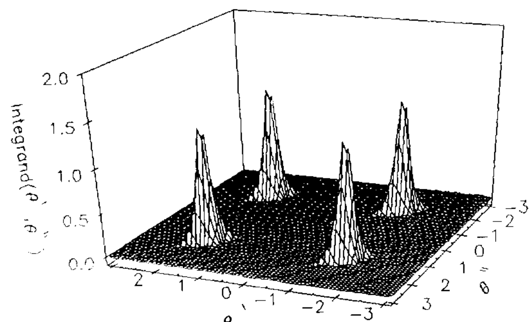

Fig.3

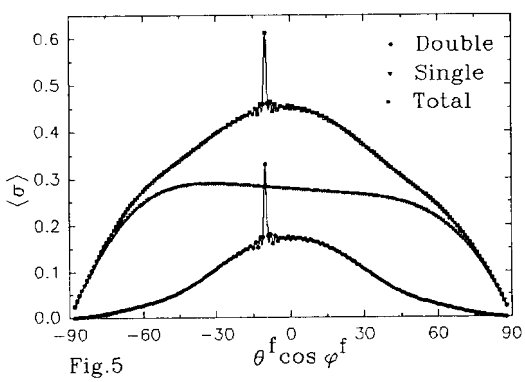

Fig.5

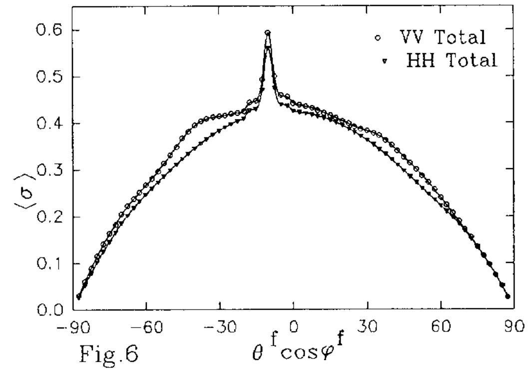

Fig.6

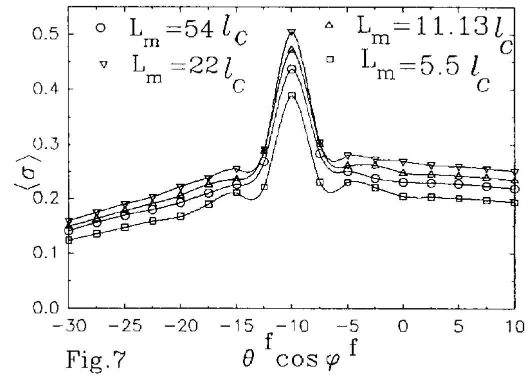

Fig.7

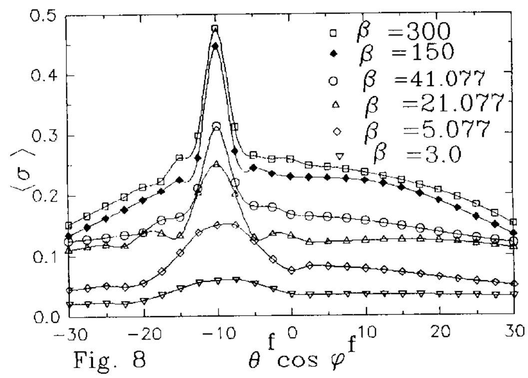

Fig. 8

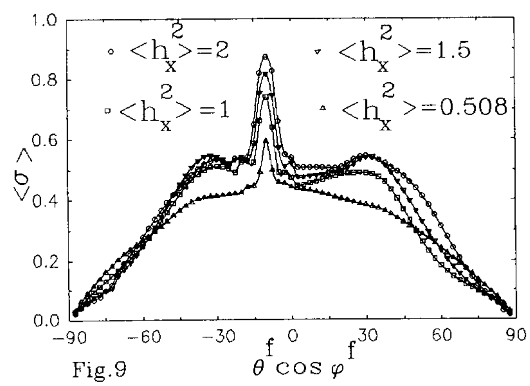

Fig.9